Structural Engineering and Mechanics, Vol. 6, No. 1 (1998) 41-61
DOI: http://dx.doi.org/10.12989/sem.1998.6.1.041

Two-dimensional nonconforming finite elements: A state-of-the-art

Chang-Koon Choi†

Dept. of Civil Engineering, Korea Advanced Institute of Science and Technology, Taejeon 305-701, Korea

Sun-Hoon Kim†

Dept. of Civil Engineering, Youngdong Institute of Technology, Youngdong 370-800, Korea

Young-Myung Park‡

Steel Structure Technology Division, Research Institute of Industrial Science and Technology, Seoul 135-777, Korea

Keun-Young Chung‡

Track structure & Environmental Division, Korea Railload Research Institute, Uiwang 437-763, Korea

Abstract. A state-of-the-art report on the new finite elements formulated by the addition of nonconforming displacement modes has been presented. The development of a series improved nonconforming finite elements for the analysis of plate and shell structures is described in the first part of this paper. These new plate and shell finite elements are established by the combined use of different improvement schemes such as; the addition of nonconforming modes, the reduced (or selective) integration, and the construction of the substitute shear strain fields. The improvement achieved may be attributable to the fact that the merits of these improvement techniques are merged into the formation of the new elements in a complementary manner. It is shown that the results obtained by the new elements give significantly improved solutions without any serious defects such as; the shear locking, spurious zero energy mode for the linear as well as nonlinear benchmark problems. Recent developments in the transition elements that have a variable number of mid-side nodes and can be effectively used in the adaptive mesh refinement are presented in the second part. Finally, the nonconforming transition flat shell elements with drilling degrees of freedom are also presented.

Key words: a state-of-the-art; nonconforming displacement modes; combined use of multiple techniques; selectively reduced integration; substitute shear strain fields; transition elements

† Professor
‡ Senior Researcher

1. Introduction

Continuous research efforts have been devoted in the recent years to the development of the more efficient and accurate finite elements (Choi 1984, Kebari and Cassel 1991, Sze and Chow 1991).

The degenerated plate/shell elements have been successfully used in a wide range of structural analysis problems, in particular for the moderately thick shells (Ahmad, *et al.* 1970). The inter-element compatibility requirement in the degenerated plate/shell elements is easily satisfied because the shape functions require only C^0 continuity (Kim and Choi 1992, Mindlin 1951). Unfortunately, however, for the thin plate/shell problems this element has one significant deficiency, i.e., the excessive flexural stiffness due to the transverse displacement constraints. The assumed displacement shape functions used in the isoparametric element constrain the element to deform in a shear mode imposing a large amount of the shearing strain in the behaviour of a plate/shell element, which causes a very slow convergence (Pawsey and Clough 1971). In addition, since the ratios of the shear stiffness and the membrane stiffness coefficients to the bending stiffness coefficients are in general the order of $(L/t)^2$ and $(L/t)^3$, respectively, the shear and membrane stiffness become to dominate the global stiffness as the thickness of the shell becomes thin (Fezans and Verchery 1982). The performance of the degenerated plate/shell elements, therefore, deteriorates rapidly in the thin plate/shell structures, and these problems are known as the shear locking and membrane locking phenomena (Parisch 1979, Tsach 1981).

In the past decade, a lot of research efforts has been directed at overcoming the locking problems in the degenerated plate/shell elements, thus rendering them effective and reliable for the thin plate/shell applications (Choi 1984, 1986, Hinton and Huang 1986, Huang and Hinton 1986, Hughes, *et al.* 1978, Lee and Wong 1982, Parisch 1979, Zienkiewicz, *et al.* 1971). As results of these research efforts, several successful remedial schemes have been suggested; namely, the reduced (or selective) integration technique (Hughes, *et al.* 1978, Pugh, *et al.* 1978, Zienkiewicz *et al.* 1971), the addition of nonconforming displacement modes (Choi 1984, Choi and Schnobrich 1975), and the use of assumed shear strain fields (Hinton and Huang 1986). Efforts have been also devoted to the development of the further improvement of plate/shell finite elements by the combined use of the aforementioned schemes (Choi 1986, Choi and Kim 1988, 1989, Choi and Yoo 1991a, Kim and Choi 1992). Thus, the evolution of the concept of combined use of nonconforming modes and other schemes, and the development of new degenerated plate/shell finite elements based on this concept are of the main concern of this paper.

The transition elements, which have a variable number of nodes in an element and are improved by the addition of nonconforming modes, have been effectively used in the adaptive mesh refinement for two dimensional problems (Choi and Park 1989, 1992, 1997, Choi and Lee 1995, 1996). The present paper addresses the state-of-the-art of the defect-free plate/shell elements developed by the addition of nonconforming displacement modes. The nonconforming transition plate/shell elements with variable mid-side nodes for local mesh refinement are also discussed.

2. Nonconforming displacement modes

2.1. Basic concepts

The approach to improve the basic behaviour of 2-D isoparametric element by eliminating

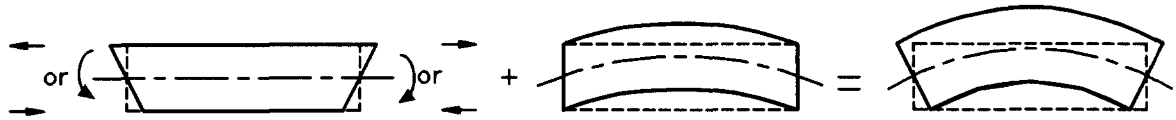

(a) constrained deformation under pure bending (b) addition of non-conforming modes (c) combined mode

Fig. 1 Restoring the actual behaviour of an element.

the excessive shear strains through the addition of nonconforming displacement modes was first adopted by Wilson, *et al.* (1971). The transverse displacement constraints which cause the excessive shear strains in the element can be eliminated by restoring the real displacement configuration with the extra modes (Fig. 1). These additional displacement modes are of the same form as the errors or what are missing in the original displacement approximation, and therefore the actual displacement field can be better approximated by the addition of these nonconforming modes.

The total displacement field of the element with additional displacement modes can be expressed as

$$[U]=\sum N_j U_j+\sum \overline{N}_j \overline{U}_j \tag{1}$$

in which $\overline{N}_j$ are the additional nonconforming modes and $\overline{U}_j$ are the additional unknowns corresponding to the additional displacement modes. These additional unknowns are not the physical nodal displacements but can be taken simply as amplitudes of the respective nonconforming modes.

The strain components in an element are expressed in a condensed form with the conforming and nonconforming parts as

$$[\varepsilon]=[\boldsymbol{B}\ \overline{\boldsymbol{B}}]\begin{bmatrix}\boldsymbol{U}\\ \overline{\boldsymbol{U}}\end{bmatrix} \tag{2}$$

Then, the element stiffness matrix can be obtained by the direct application of variational principles. The resulting stiffness matrix has been enlarged over the original isoparametric element matrix due to the additional modes and the corresponding unknowns and partitioned as

$$\begin{bmatrix}\boldsymbol{K}_{cc} & \boldsymbol{K}_{cn}\\ \boldsymbol{K}_{cn}{}^{T} & \boldsymbol{K}_{nn}\end{bmatrix}\begin{bmatrix}\boldsymbol{U}\\ \overline{\boldsymbol{U}}\end{bmatrix}=\begin{bmatrix}\boldsymbol{F}\\ 0\end{bmatrix} \tag{3}$$

where

$$\boldsymbol{K}_{cc}=\int_V \boldsymbol{B}^T\boldsymbol{D}\boldsymbol{B}dV,\qquad \boldsymbol{K}_{cn}=\int_V \boldsymbol{B}^T\boldsymbol{D}\overline{\boldsymbol{B}}dV,\qquad \boldsymbol{K}_{nn}=\int_V \overline{\boldsymbol{B}}^T\boldsymbol{D}\overline{\boldsymbol{B}}dV \tag{3a}$$

and c denotes conforming whereas n denotes nonconforming part. The null vector in the lower part of the load vector in Eq. (3) indicates that no nodal loads can be applied in association with the nonconforming modes.

The enlarged element stiffness matrix in Eq. (3) can be condensed back to the same size as the stiffness matrix of the ordinary degenerated plate and shell elements as (Choi and Schnobrich 1975, Taylor, *et al.* 1976)

$$K'U=(K_{cc}-K_{cn}K_{nn}^{-1}K_{cn}^{T})\ U=F \tag{4}$$

The applications of the aforementioned approach and its modified versions could be found in the plane stress/strain and axisymmetric problems (Choi and Kim 1989, Cook 1972, 1974, 1975, Taylor, *et al.* 1976, Wilson *et al.* 1971). Through various numerical studies, Choi, *et al.* (1989) showed that the nonconforming elements behave much better than the conforming elements when in particular the irregular meshes are used. Cochet and Dhatt (1978) also showed that the nonconforming plane element gave the efficient solutions for an estimation of collapse loads in plasticity problems.

2.2. Formulations of nonconforming plate/shell elements

Almost parallel to the application into the in-plane stress/strain problems, the degenerated shell element which utilizes the concept of restoring the real deformation by the addition of nonconforming modes was first proposed by Choi and Schnobrich (1975). The possible nonconforming displacement modes to be added to a 4-node degenerated shell element and an 8-node serendipity shell element are defined by the following set of shape functions (Choi and Schnobrich 1975) in Eq. (5) and in Eq. (6), respectively.

$$\begin{aligned}&\overline{N}_1=(1-\xi^2),\quad \overline{N}_2=(1-\eta^2),\quad \overline{N}_3=\eta(1-\xi^2)\\&\overline{N}_4=\xi(1-\eta^2),\quad \overline{N}_5=(1-\xi^2)(1-\eta^2)\end{aligned} \tag{5}$$

$$\begin{aligned}&\overline{N}_1=\xi(1-\xi^2),\ \overline{N}_2=\eta(1-\eta^2),\quad \overline{N}_3=\xi\eta(1-\xi^2)\\&\overline{N}_4=\xi\eta(1-\eta^2),\quad \overline{N}_5=(1-\xi^2)(1-\eta^2)\end{aligned} \tag{6}$$

The additional modes in Eq. (5) and (6) are selected to have zero values at each node and

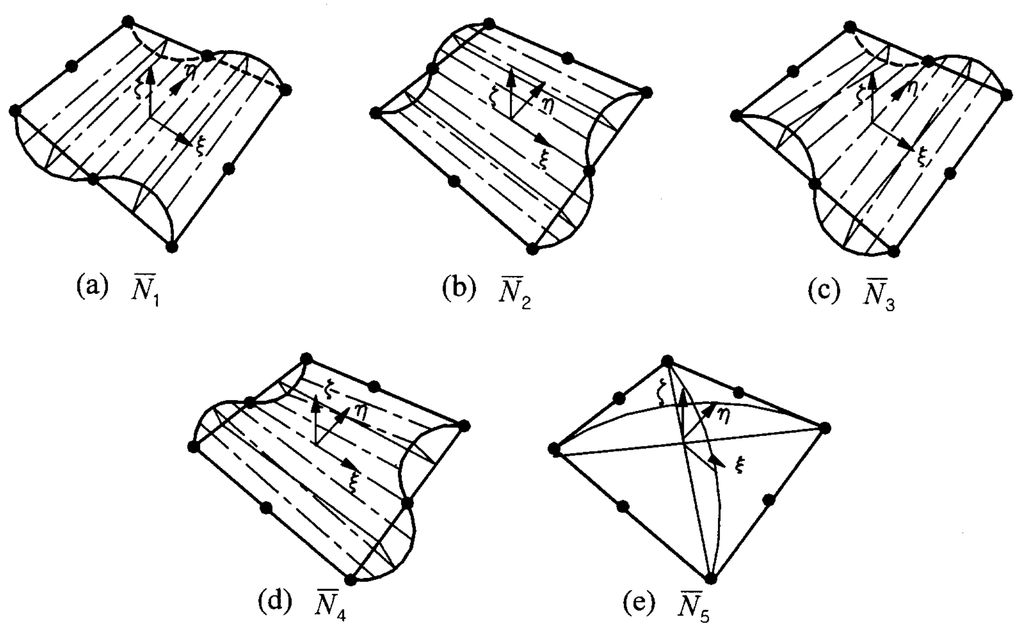

Fig. 2 Non-conforming displacement modes in quadratic element.

to eliminate the undesirable constraints present in an original isoparametric element. The first two modes in Eq. (5) and (6) are to eliminate the transverse displacement constraints and the third and fourth modes contribute to the softening of twisting constraints. The fifth mode adds the bubble shape displacement in the element (Fig. 2).

The displacement fields of a nonconforming degenerated plate element and a nonconforming shell element can be formed by adding nonconforming displacement components to the original displacement of the element as given in Eq. (7) and Eq. (8), respectively (Choi and Schnobrich 1975, Choi 1982).

$$\begin{bmatrix} u \\ v \\ w \end{bmatrix} = \sum N_i \begin{bmatrix} z\theta_{xi} \\ z\theta_{yi} \\ w_i \end{bmatrix} + \sum \overline{N}_j \begin{bmatrix} z\overline{\theta}_{xj} \\ z\overline{\theta}_{yi} \\ \overline{w}_j \end{bmatrix} \tag{7}$$

$$\begin{bmatrix} u \\ v \\ w \end{bmatrix} = \sum N_i \begin{bmatrix} u_i \\ v_i \\ w_i \end{bmatrix} + \sum N_i \frac{t}{2} \zeta \phi_i \begin{bmatrix} \alpha_i \\ \beta_i \end{bmatrix} + \sum \overline{N}_j \begin{bmatrix} \overline{u}_j \\ \overline{v}_j \\ \overline{w}_j \end{bmatrix} \tag{8}$$

where θ_{xi} and θ_{yi} are the rotations in the xz and yz planes at node i due to the plate bending, respectively, ϕ_i is the direction cosine matrix at node i, α_i and β_i are two nodal rotations. It should be noted that no rotational nonconforming modes are added in Eq. (8).

By the selective combinations of shape functions, Choi and Schnobrich (1975) established a series of nonconforming plate/shell elements. Based on their investigations with several types of structures using various combinations of nonconforming modes, it was observed that the improvement obtained for 4-node element was more significant (See Fig. 3 and Fig. 4) than that for 8-node element. However, since the 4-node element still need to be improved further to become an effective element for the practical use, the research efforts are naturally focused on the 8-node nonconforming elements.

2.3. Selective addition of nonconforming modes

Since the addition of nonconforming modes inevitably requires increased computational efforts, it is therefore desirable to minimize the number of added nonconforming modes without significant sacrifice in the accuracy of obtainable solutions. Choi (1984) suggested for his quadratic plate/shell element that the additions to in-plane displacement components might be dropped while nonconforming modes added to transverse displacement components should be retained since the errors associated with the in-plane displacement in a quadratic element are much less significant than the transverse displacement. This scheme, which is the earliest and simplest modification made to the general nonconforming element concept, is more effective for the higher order elements for which the displacements are already expressed by higher order functions.

The displacement fields of a degenerated plate element and a shell element which are simplified in accordance with the above discussion are now expressed as in Eq. (9) and Eq. (10), respectively.

$$\begin{bmatrix} u \\ v \\ w \end{bmatrix} = \sum N_i \begin{bmatrix} z\theta_{xi} \\ z\theta_{yi} \\ w_i \end{bmatrix} + \sum \overline{N}_j \begin{bmatrix} 0 \\ 0 \\ \overline{w}_j \end{bmatrix} \tag{9}$$

$$\begin{bmatrix} u \\ v \\ w \end{bmatrix} = \sum N_i \begin{bmatrix} u_i \\ v_i \\ w_i \end{bmatrix} + \sum N_i \frac{t}{2} \zeta \phi_i \begin{bmatrix} \alpha_i \\ \beta_i \end{bmatrix} + \sum \overline{N}_j \begin{bmatrix} 0 \\ 0 \\ \overline{w}_j \end{bmatrix} \tag{10}$$

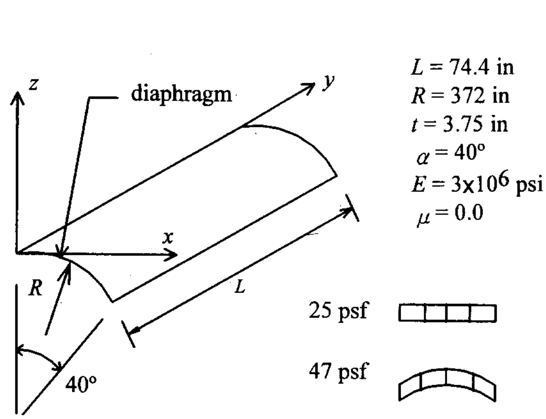

Fig. 3 Geometry and material properties of circular cylindrical shell.

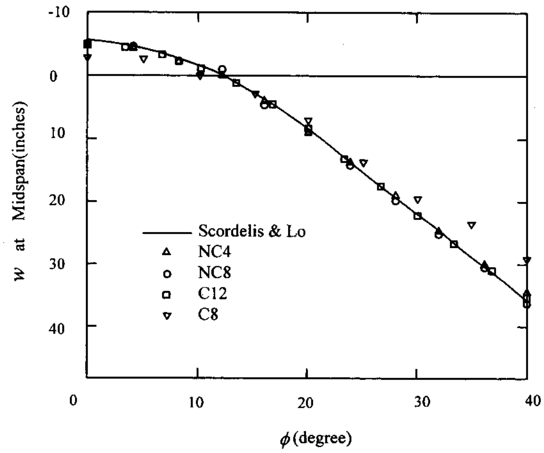

Fig. 4 Displacement for circular cylindrical shell under uniform load.

A similar performance of these simplified nonconforming elements in Eqs. (9) and (10) as that of the original nonconforming elements in Eqs. (7) and (8) has been reported (Choi 1984). This fact can be explained by the basis of discrete Kirchhoff mode criterion (Hughes and Tezduyar 1981, Kim and Choi 1988). Since the transverse displacement is interpolated with one order higher functions than rotations due to the addition of nonconforming modes, this simplification may give satisfaction of the discrete Kirchhoff mode expressed by

$$\gamma_{xz}=\theta_x+\partial w/\partial x=0, \qquad \gamma_{yz}=\theta_y+\partial w/\partial y=0 \tag{11}$$

3. Improvement of plate/shell elements

In parallel to the development of schemes for nonconforming elements, the reduced integration techniques are also used to improve the original degenerated element (Choi, *et al.* 1986, 1988, 1989, 1991, 1992, Pugh, *et al.* 1978). The coupled use of addition of nonconforming modes and other improvement techniques in a complementary way may further increase the effectiveness and versatility of the element. An element can avoid the shear locking phenomenon when the interpolated shear strain function contains more variables than the number of equations obtained when equating the shear strain to zero (Tsach 1981). Since the number of shear strain constraints can be reduced by the use of reduced integration and the number of variables can be increased by the addition of nonconforming modes, the coupled use of these two schemes is thus effective to avoid shear locking (Kim and Choi 1992).

3.1. Selective nonconforming modes and selective integration

The combined use of the reduced integration and the addition of nonconforming modes can be implemented rather simply by integrating each of the sub-matrices in Eq. (3) with reduced orders. However, for the element that has all five nonconforming mode shapes in Eq. (6), a uniform reduction of the integration order resulted in obtaining a singular matrix. In order to avoid this difficulty, different orders of integration for the sub-matrices in Eq. (3), i.e., 2×2 integration for K_{cc} and K_{cn}, and 3×3 rule for K_{nn}, are suggested (Choi 1986) for the element stiffness formulation based on the displacement fields in Eq. (10). These elements do not possess any spurious zero energy mode and gave improved results but produced locking phenomena in thin plates and shells. The spurious zero energy mode can be avoided for these element by applying the normal integration to the stiffness sub-matrix K_{nn} that has same effects as multiplying K_{nn} by a factor $(1+e)$ as suggested by Cook (1972). The latter, however, requires some experiences in deciding the optimal value of an artificial factor $(1+e)$ (Kim and Choi 1992).

It was found that the terms in the stiffness matrix pertinent to the nonconforming mode shapes N_1 and N_2 become zeros because the derivatives of these shape functions vanish (i.e., $\overline{N}_{1,\xi}=\overline{N}_{1,\eta}=\overline{N}_{2,\xi}=\overline{N}_{2,\eta}=0$) when computed at the reduced integration points (i.e., $\xi=\pm 1/\sqrt{3}$, $\eta=\pm 1/\sqrt{3}$). Therefore, addition of these two nonconforming modes is of no consequences when reduced integration is applied. This will explain why the uniformly reduced integration resulted in obtaining a singular matrix as stated above. It is also noted that the derivatives of $\overline{N}_3$ and $\overline{N}_4$ with respect to ξ and η, respectively, are zeros ($\overline{N}_{3,\xi}=\overline{N}_{4,\eta}=0$) when integrated with reduced order, but note that $\overline{N}_{3,\eta}\neq 0$ and $\overline{N}_{4,\xi}\neq 0$. Therefore, their overall contribution to the element stiffness may not be significant. Thus, based on the displacement field of Eq. (9) and Eq. (10), two other types of the reduced integrated nonconforming plate/shell elements, i.e., elements designated as NC8-A and NC8-B which have three ($\overline{N}_3$, $\overline{N}_4$, $\overline{N}_5$) or one ($\overline{N}_5$) nonconforming modes, respectively, are developed (See Table 1, Choi and Kim 1988). These elements give good results in plate/shell problems, but because of the rank deficiency of their stiffness matrices the elements possess spurious zero energy modes which can contaminate the solution (See Table 1 and Fig. 5).

3.2. Coupled use of nonconforming modes and reduced Integration

In order to overcome the aforementioned problems of the shear locking phenomenon and the spurious zero energy modes, further improved degenerated plate elements are suggested (Choi and Kim 1989). As the first step, the overall element stiffness was separated into the stiffness pertinent to bending and shear, and then, the nonconforming displacement modes are added only to the shear stiffness while no nonconforming modes are added to the bending stiffness.

The strain components of the degenerated plate element are expressed in the following form.

$$[\varepsilon]=\sum\begin{bmatrix} \boldsymbol{B}_{bi} \\ \boldsymbol{B}_{si} \end{bmatrix}\begin{bmatrix} \theta_{xi} \\ \theta_{yi} \\ w_i \end{bmatrix}+\sum\begin{bmatrix} \boldsymbol{0} \\ \overline{\boldsymbol{B}}_{sj} \end{bmatrix}\begin{bmatrix} 0 \\ 0 \\ \overline{w}_j \end{bmatrix} \tag{12}$$

where

$$[\boldsymbol{B}_{bi}]=\begin{bmatrix} N_{i,x} & 0 & 0 \\ 0 & N_{i,y} & 0 \\ N_{i,y} & N_{i,x} & 0 \end{bmatrix},\quad [\boldsymbol{B}_{si}]=\begin{bmatrix} N_i & 0 & N_{i,x} \\ 0 & N_i & N_{i,y} \end{bmatrix},\quad [\overline{\boldsymbol{B}}_{sj}]=\begin{bmatrix} 0 & 0 & \overline{N}_{i,x} \\ 0 & 0 & \overline{N}_{i,y} \end{bmatrix} \tag{12a}$$

In the evaluation of shear stiffness of an element with nonconforming displacement mode, the normal order Gaussian quadrature (3×3 integration) is used since the reduced integration for the shear stiffness may cause spurious zero energy modes (Choi and Kim 1988) while the bending stiffness is computed with a reduced integration order (2×2 integration).

Indicating the integration orders by numbers in the parenthesis, the final element stiffness matrix $\boldsymbol{K}^e$ is computed by the following scheme.

Table 1 Quadratic degenerated plate element

Reference	Element ID	Shape Functions for Displacement Components		Integration Scheme						DOF/Element Before/After Condensation	Number of Zero Eignvalue	
				K_{CC}		K_{CN}		K_{NN}				
		w	θ_x, θ_y	B	S	B	S	B	S		Total	Spurious
Pugh, *et al.* (1978)	QSR	8-node	8-node	R	R	-	-	-	-	24/24	4	1*
Hughes, *et al.* (1978)	QLS	9-node	9-node	N	R	-	-	-	-	27/27	4	1
Hughes and Cohen(1978)	QHS	8-node	9-node	N	R	-	-	-	-	26/26	3	0
Choi(1986)	NC8-4.1	8-node+$\bar{N}_1 \sim \bar{N}_4$	8-node	R	R	R	R	N	N	28/24	3	0
	NC8-4.2	8-node+$\bar{N}_1 \sim \bar{N}_5$	8-node	R	R	R	R	N	N	29/24	3	0
Choi and Kim (1988)	NC8-A	8-node+$\bar{N}_3 \sim \bar{N}_5$	8-node	R	R	R	R	R	R	27/24	7	4
	NC8-B	8-node+$\bar{N}_5$	8-node	R	R	R	R	R	R	25/24	5	2
Choi and Kim (1989)	NC8-AS	8-node+$\bar{N}_3 \sim \bar{N}_5$	8-node	R	N	-	N	-	N	27/24	3	0
	NC8-BS	8-node+$\bar{N}_5$	8-node	R	N	-	N	-	N	25/24	3	0
	NC8-CS	8-node+$\bar{N}_1 \bar{N}_2 \bar{N}_5$	8-node	R	N	-	N	-	N	27/24	3	0
	NC8-DS	8-node+$\bar{N}_1 \sim \bar{N}_5$	8-node	R	N	-	N	-	N	29/24	3	0
Kim and Choi (1992)	NC-QH	8-node	8-node +$\bar{N}_1 \bar{N}_2 \bar{N}_5$	N	R	N	R	N	R	30/24	3	0

R: Reduced Integration (2×2)
N: Normal Integration (3×3)
*: Not communicable in a mesh of two or more elements
S: shear part of stiffness matrix
B: Bending part of stiffness matrix

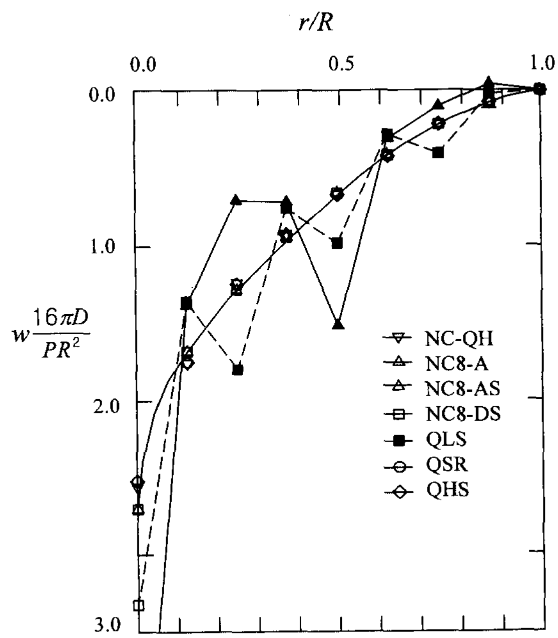

Fig. 5 Displacement results for thick circular plate (R/t=2.5).

$$\boldsymbol{K}^e=\boldsymbol{K}^e_{b(2\times 2)}+\boldsymbol{K}^e_{s(3\times 3)} \tag{13}$$

where

$$\boldsymbol{K}^e_{b(2\times 2)}=\int_V [\boldsymbol{B}_b']^T[\boldsymbol{D}_b][\boldsymbol{B}_b']dV, \qquad \boldsymbol{K}^e_{s(3\times 3)}=\int_V [\boldsymbol{B}_s']^T[\boldsymbol{D}_s][\boldsymbol{B}_s']dV \tag{13a}$$

$$[\boldsymbol{B}_b']=[\boldsymbol{B}_b\ \ 0], \qquad [\boldsymbol{B}_s']=[\boldsymbol{B}_s\ \ \overline{\boldsymbol{B}}_s] \tag{13b}$$

Based on the detailed versions of Eq. (13), the establishment of a series of new degenerated plate elements are proposed (Choi and Kim 1989). The element has been designated as NC8-AS which is a selectively integrated version of NC8-A. The element has three additional modes ($\overline{N}_3$, $\overline{N}_4$ and $\overline{N}_5$) applied only to the transverse displacement (w) and the stiffness is obtained by the selective integration. The elements designated as NC8-BS, NC8-CS and NC8-DS are established in a similar manner. These elements have one ($\overline{N}_5$), three ($\overline{N}_1$, $\overline{N}_2$ and $\overline{N}_5$) and five nonconforming modes ($\overline{N}_1 \sim \overline{N}_5$), respectively (See Table 1). The behavior of the elements has been improved and the degeneracy in the accuracy of the distorted element and the shear locking phenomenon (in the regular mesh) do not exist any longer. The elements do not possess any spurious zero energy modes either (See Table 1 and Fig. 5). These elements also passed the patch test (See Table 2 and Fig. 6).

3.3. Coupling of nonconforming modes to rotations and reduced Integration

The two major problems associated with the coupled use of reduced integration and addition of nonconforming modes are; 1) the singularity of the derivatives of the nonconforming shape functions and 2) the occurrence of spurious zero energy modes when the full reduced integration is used for nonconforming element(Choi and Kim 1988).

The addition of nonconforming modes to rotational displacements (θ_x, θ_y) does not require the derivatives of nonconforming shape functions for the calculation of the stiffness matrix in the degenerated plate elements. Thus, the first problem can be solved easily by this approach. The second difficulty which is associated with the rank deficiency of the element stiffness matrix can be avoided by the selective integration technique in which the bending and shear parts of element stiffness are computed with different integration order, i.e., 3×3 integration for bending and 2×2 integration for shear (Kim and Choi 1992). The displacement field in a new degenerated plate element can be expressed by

$$\begin{bmatrix} u \\ v \\ w \end{bmatrix}=\sum N_i \begin{bmatrix} z\theta_{xi} \\ z\theta_{yi} \\ w_i \end{bmatrix}+\sum \overline{N}_j \begin{bmatrix} z\overline{\theta}_{xj} \\ z\overline{\theta}_{yi} \\ 0 \end{bmatrix} \tag{14}$$

Based on the expression in Eq. (14), the establishments of various new elements are possible. The element which has three nonconforming modes ($\overline{N}_1$, $\overline{N}_2$ and $\overline{N}_5$) applied to the rotational displacement and uses the selective integration scheme for the calculation of the element stiffness has shown neither the shear locking phenomenon for both the irregular and regular meshes nor the spurious zero energy modes (Kim and Choi 1992). This element has been designated as NC-QH which indicates "Non-Conforming Quadratic Heterosis" element because the QHS element (Hughes and Cohen 1978) can be achieved by adding a bubble mode ($\overline{N}_5$) only to the rotational displacements of the 8-node element. The NC-QH element does not pass the Irons' patch test (Table 2), but passes the weak patch test which uses a sequence of refined

Table 2 Summary of patch test

Element \ Case	Bending	Shearing	Twisting	Remarks
QSR	fail	pass	fail	fail
QLS	pass	pass	pass	fail
QHS*	fail	fail	fail	fail
NC8-AS	pass	pass	pass	pass
NC8-BS	pass	pass	pass	pass
NC8-CS	pass	pass	pass	pass
NC8-DS	pass	pass	pass	pass
NC-QH*	fail	fail	fail	fail
NC8-DC	fail	fail	fail	fail
NC8-CC	fail	fail	fail	fail

*pass the weak patch tests (Park and Choi 1997)

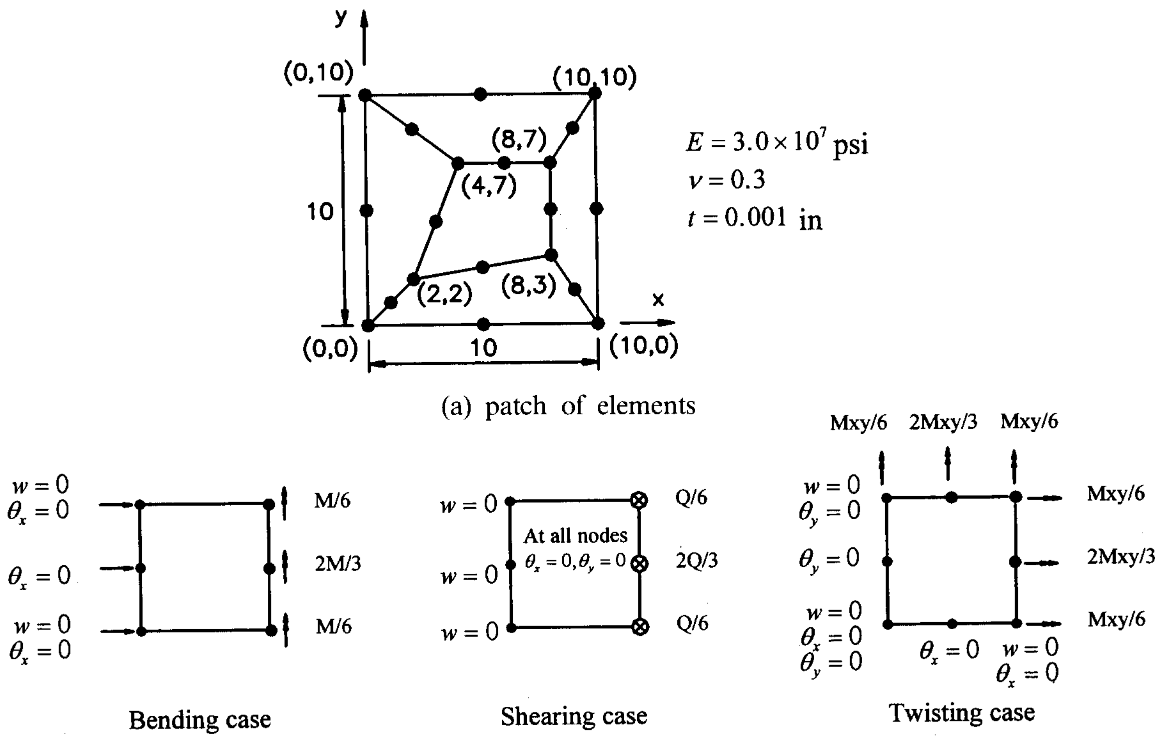

(a) patch of elements

(b) load cases

Fig. 6 Mesh patterns for patch test.

meshes in Fig. 7 and the convergence is guaranteed (Park and Choi 1997).

Table 3 shows the behaviors of some typical quadratic Mindlin plate elements, i.e. the fully reduced integrated 8-node element QSR (Pugh, *et al.* 1978), selectively integrated 9-node element QLS (Hughes, *et al.* 1978), and heterosis element QHS (Hughes and Cohen 1978). Although the NC-QH element and the heterosis element (QHS) give the similar behavior in the plate bending problem with the regular mesh, the former is superior over the other elements studied for the problem with irregular mesh (See Table 3 and Fig. 8) (Kim and Choi 1992, Lee and Wong 1982).

3.4. Reduced integrated nonconforming modes and substitute shear strain

In the formulation of the degenerated shell elements, research continued to establish even better elements by the use of several schemes simultaneously (Choi and Yoo 1991a). The overall element stiffness is separated into the transverse shear stiffness and the in-plane stiffness (i.e., the combined effects of the membrane and bending actions) at first. Then, the substitute shear strain fields are formulated by interporating the values at sampling points. Locations of the sampling points for the substitute shear strain fields are the points where each of the transverse shear strain becomes zero for very thin plate/shell in an average sense (Hinton and Huang 1986) so that the shear locking problems can be eliminated . In the case of in-plane stiffness, the stiffness is computed with reduced integration (i.e., 2×2 integration) to avoid the membrane locking problems. In addition, the nonconforming displacement modes are added to the translational displacement components to improve the overall performance of the element. In the evaluation of transverse shear stiffness of an element, the 2×3 integration in one direction and 3×2 in the other direction is used while the in-plane stiffness is computed with the single reduced integration order (see Table 4, Huang and Hinton 1986).

The relationship between strain and the displacements for the element formulation is expressed as

$$\varepsilon = \boldsymbol{B}\boldsymbol{U}_t = \sum \begin{bmatrix} \boldsymbol{B}_f \\ \widetilde{\boldsymbol{B}}_s \end{bmatrix} U + \sum \begin{bmatrix} \overline{\boldsymbol{B}}_f \\ \overline{\boldsymbol{B}}_s \end{bmatrix} \overline{U} \tag{15}$$

where $\boldsymbol{U}=[u,\ v,\ w,\ \alpha,\ \beta]^T$, $\overline{\boldsymbol{U}}=[\overline{u},\ \overline{v},\ \overline{w},\ \overline{\alpha},\ \overline{\beta}]^T$. $\boldsymbol{B}_f$ is the strain-displacement matrix of in-plane displacement, $\widetilde{\boldsymbol{B}}_s$ is that of the substitute shear displacement, $\overline{\boldsymbol{B}}_f$ and $\overline{\boldsymbol{B}}_s$ are those related to nonconforming displacement modes, and $\overline{U}$ is the additional degrees of freedom corresponding to the nonconforming displacement mode.

Based on Eq. (15), two new types of elements, namely, NC8-DC and NC8-CC are developed.

Table 3 Results of shear locking test for clamped square plates subjected to uniform load (NEL=16); normalized values of maximum transverse displacement

Mesh Type	Regular mesh			Irregular mesh			Remarks
Element \ t/L	10^{-1}	10^{-2}	10^{-4}	10^{-1}	10^{-2}	10^{-4}	
QSR	1.505	1.259	0.122	1.505	1.242	0.011	fail
QLS	1.505	1.268	1.266	1.506	1.264	1.236	pass
QHS	1.505	1.264	1.257	1.505	1.257	0.457	fail
NC8-AS	1.491	1.205	1.195	1.492	1.187	0.038	fail
NC8-BS	1.490	1.205	1.195	1.493	1.186	0.030	fail
NC8-CS	1.496	1.260	1.195	1.500	1.247	0.052	fail
NC8-DS	1.496	1.267	1.196	1.500	1.267	0.384	fail
NC-QH	1.505	1.267	1.265	1.506	1.267	1.263	pass
Theory	1.500*	1.265		1.500*	1.265		

*Thick plates which include shear deformation

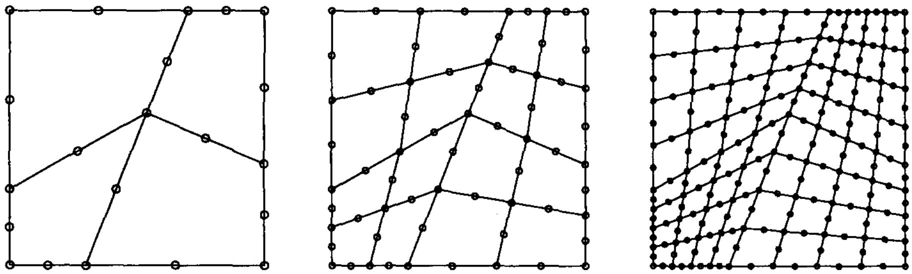

(a) 2×2 (b) 4×4 (c) 8×8 mesh

Fig. 7 Weak patch model.

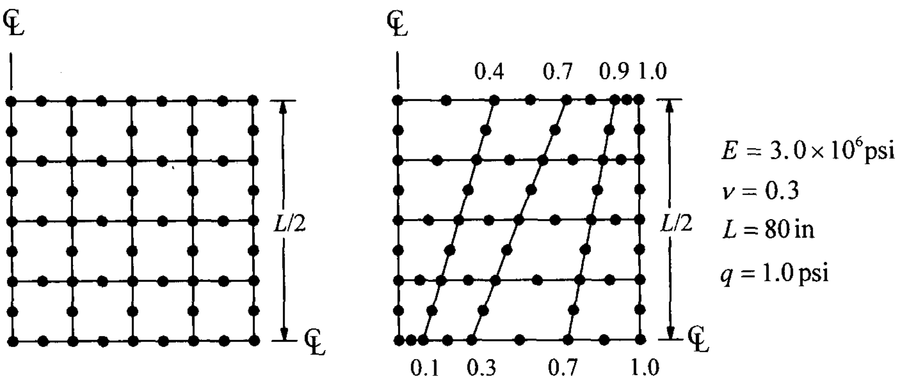

(a) regular mesh (b) irregular mesh

Fig. 8 Square plate models.

The last letter C indicates "Combined use of improvement schemes".

It is shown that the results obtained by these two elements give reliable solutions without any defects for the linear and nonlinear benchmark problems (See Table 5 and Figs. 9 and 10, Choi and Yoo 1991b).

4. Nonconforming transition elements

For an efficient analysis of the structures that have non-uniform stress distribution, it is a usual practice to use a finer finite element grid in the area of the higher stress gradients. The variable node transition element which has mid-side nodes, can be used effectively to connect the rather coarser grid to the finer grid (Fig. 11). The behavior of this variable node element has been improved also through addition of modified nonconforming modes in a similar way (Choi and Park 1989, 1997, Choi 1992, Choi and Lee 1995).

4.1. Plane stress elements

To ensure the compatibility of the sides where two 4-node elements are connected to one side of the transition element with mid-side node (Fig. 11), a special shape functions with the slope discontinuity at the mid-side node are used as in Eq. (16).

Table 4 Quadratic degenerated shell element

Reference	Element Name	Shape Function for Displacement Componeent: u,v,w	Shape Function for Displacement Componeent: α,β	Stiffness	Integration Scheme — Conforming Shape Functions: $N_1 \sim N_8$ (u,v,w,α,β)	Nonconforming Shape Functions: $\bar{N}_5$ ($\bar{u}$)	$\bar{N}_5$ ($\bar{v}$)	$\bar{N}_5$ ($\bar{w}$)	$\bar{N}_1$, $\bar{N}_2$ ($\bar{u},\bar{v},\bar{w}$)	$\bar{N}_3$, $\bar{N}_4$ ($\bar{u},\bar{v},\bar{w}$)	DOF/Element: Before/After Condensation	Number of zero Eigenvalues: Total	Spurious modes
Zienkiewicz (1971)	QSR	8-node	8-node	In-plane	R	-	-	-	-	-	40/40	8	2*
				Shear	R	-	-	-	-	-			
Parisch (1979)	QLR	9-node	9-node	In-plane	R	-	-	-	-	-	45/45	13	5+2*
				Shear	R	-	-	-	-	-			
	QLS	9-node	9-node	In-plane	N	-	-	-	-	-	45/45	9	2+1*
				Shear	R	-	-	-	-	-			
	QLN	9-node	9-node	In-plane	N	-	-	-	-	-	45/45	6	0
				Shear	N	-	-	-	-	-			
Choi and Yoo(1991a)	NC8-DC	8-node	8-node	In-plane	R	R	R	R	N	N	55/40	7	1*
		$+\bar{N}_1 \sim \bar{N}_5$		Shear	M	N	N	M	N	N			
	NC8-CC	8-node	8-node	In-plane	R	R	R	R	N	-	49/40	7	1*
		$+\bar{N}_1\bar{N}_2\bar{N}_5$		Shear	M	N	N	M	N	-			

R: Reduced integration (2×2)
N: Normal integration (3×3)
M: Modified integration (2×3/3×2)
*: Not Communicable in a mesh of two or more elements

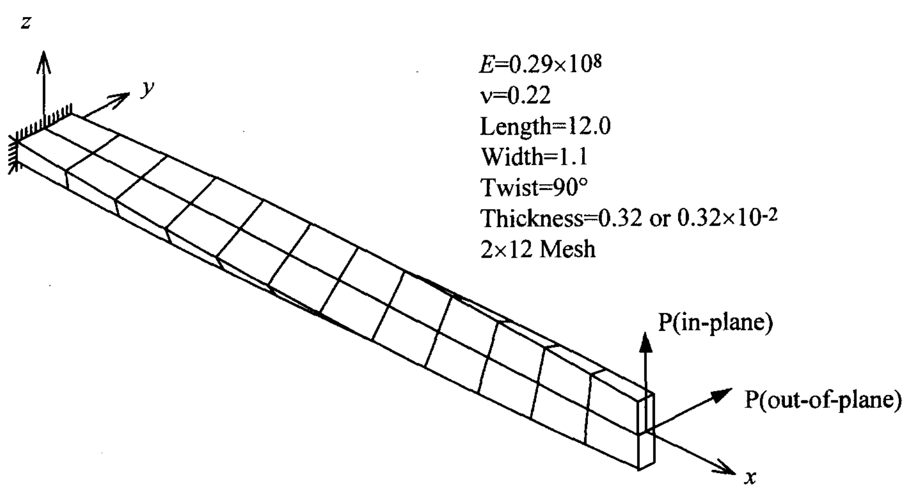

Fig. 9 Twisted beam subjected concentrated load at tip.

$$N_1 = N_1' - \frac{1}{2} N_5, \qquad N_2 = N_2' - \frac{1}{2}(N_5 + N_6), \qquad N_3 = N_3' - \frac{1}{2} N_6,$$

$$N_4 = N_4', \qquad N_5 = \frac{1}{2}(1 - |\xi|)(1 - \eta), \qquad N_6 = \frac{1}{2}(1 + \xi)(1 - |\eta|) \tag{16}$$

where,

Table 5 Normalized solution for twisted beam

Thickness	Thick(t=0.32)		Thin(t=0.0032)	
Element \ Load Case	In-Plane	Out-of-Plane	In-Plane	Out-of-Plane
QLR	0.5424	0.1754	0.5309	0.1294
QLS	0.5370	0.1736	0.0105	0.0039
QLN	0.5316	0.1719	0.0053	0.0013
NC8-DC	0.5424	0.1772	0.5256	0.1294
NC8-CC	0.5424	0.1754	0.5203	0.1294
Beam Theory	0.5424	0.1754	0.5256	0.1294

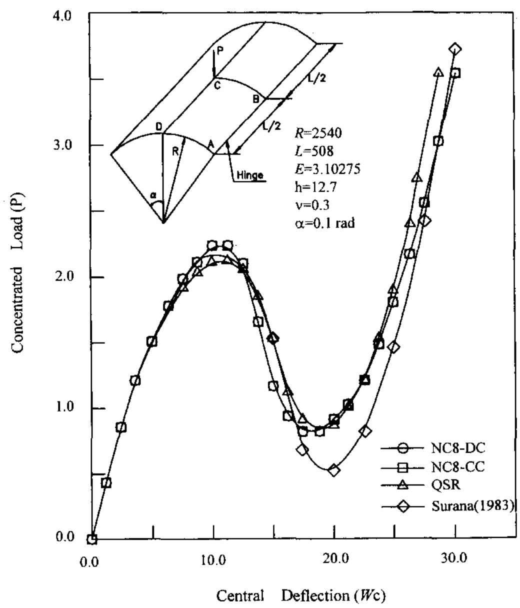

Fig. 10 Load-deflection relation for hinged cylindrical shell subjected to concentrated load.

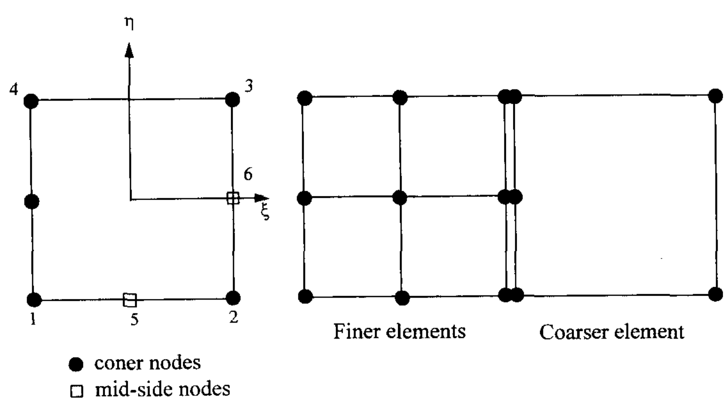

Fig. 11 Configuration and usage of transition element.

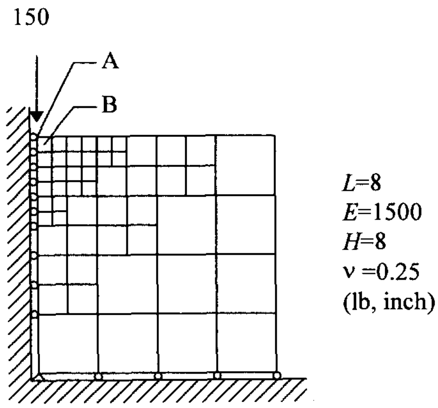

Fig. 12 Locally refined mesh for semi-infinite elasticity problem.

Table 6 Test result for semi-infinite elasticity problem

Element and mesh	References	Number of elements	Vertical deflection at A	Vertical stress at B
C4+C5+C6	Gupta (1978)	52	0.6513	−574.7
NC4+NC5+NC6	Choi (1992)	52	0.6791	−630.1
NC4	Bathe, *et al.* (1974)	1024	0.6857	−631.5

$$N_i' = \frac{1}{4}(1+\xi_i\xi)(1+\eta_i\eta), \text{ for } i=1,\ 2,\ 3,\ 4 \tag{16a}$$

In order to improve the behavior of the elements, the special nonconforming displacement modes in Eq. (17) are added to the original displacement fields.

$$\begin{aligned} &\bar{N}_1=(1-\xi^2), \quad \bar{N}_2=(1-\eta^2), \\ &\bar{N}_3=(1-\xi^2)-(1-|\xi|)(1-\eta)/2, \quad \bar{N}_4=(1-\eta^2)-(1+\xi)(1-|\eta|)/2 \end{aligned} \tag{17}$$

Considering the slope discontinuity in the domain of transition element, the modified quadrature formula was used to numerically integrate the stiffness matrix (Gupta 1978, Choi and Park 1992).

The inplane transition elements developed do not produce any spurious zero energy modes. The accuracy and applicability of the transition elements to local mesh refinement for an efficient solution of a plane stress problem was shown in the semi-infinite elasticity problem under a concentrated load (See Fig. 12). The results obtained by the nonconforming transition model (Choi 1992) is better than that obtained by the conforming model (Gupta 1978). The solution by 1024 nonconforming 4-node elements (Bathe, *et al.* 1974) is given as a reference solution (See Table 6).

4.2. Plate bending elements

For the formulation of the variable node transition plate bending element which is based on the Reissner-Mindlin plate theory, the shape functions for the mid-side nodes are written as

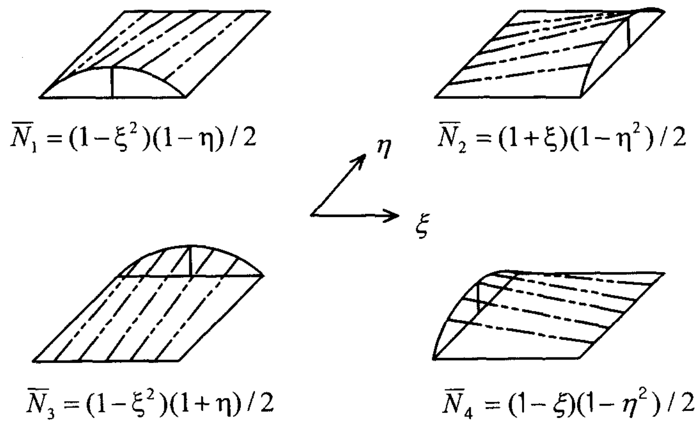

Fig. 13 Non-conforming modes for transition plate bending element.

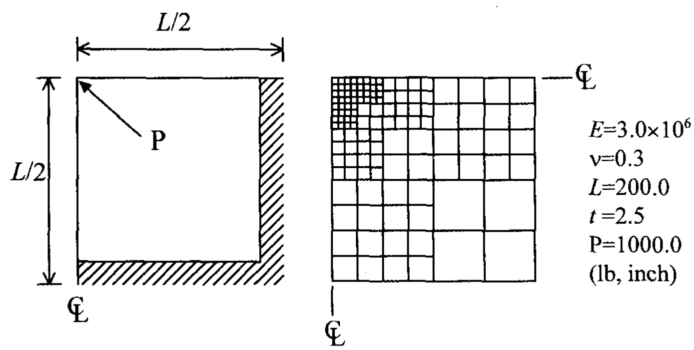

(a) Configuration (b) Locally refined mesh

Fig. 14 Clamped square plate; A quarter model.

Table 7 Test result for clamped square plate

Element and mesh	Reference	Number of elements	Vertical deflection*
C4+C5+C6**	-	124	0.0185403
NC4+NC5+NC6	Choi and Park (1989)	124	0.0524307
Thin plate/shell			
HCT(16×16)	Clough, *et al.* (1968)	256	0.0521213
Thin plate theory	Timoshenko (1959)	—	0.0521830

*Deflection at loaded point

**This variable node plate element is formulated without non-conforming modes

$$N_5 = \frac{1}{2}(1-\xi^2)(1-\eta), \qquad N_6 = \frac{1}{2}(1+\xi)(1-\eta^2) \tag{18}$$

and the same shape function in Eqs. (16) and (16a) are used for the four corner nodes. For the element sides with mid-side nodes, the curved deformation is already expressed by the original shape functions. Therefore, it is desirable to add the nonconforming modes to the sides without any mid-side nodes so that the deformations in an element can be consistent. Thus, the nonconforming displacement modes shown in Fig. 13 are selectively added to the 5-node and 6-node transition elements, and also to the regular 4-node element. The nonconforming displacement modes are added only to the transverse displacement (w) mainly to remedy the excessive shear strains in the direction of thickness (Choi and Park 1989). The added nonconforming modes are $\bar{N}_1 \sim \bar{N}_4$ for 4-node element, $\bar{N}_2 \sim \bar{N}_4$ for 5-node element, and $\bar{N}_3$ and $\bar{N}_4$ for 6-node element and the normal 2×2 Gaussian quadrature is used for evaluation of the individual element matrices.

To show the effectiveness of these transition elements for plate bending problems, a clamped square plate under a concentrated load at the center was tested (See Fig. 14(a), (b)) and the test results are listed in Table 7. The accuracy of results is satisfactory when compared with the results by HCT (16×16 thin plate/shell element, Clough and Johnson 1968) where a larger number of elements in the HCT model (256 elements) is used compared with a small number of elements in the transition model (124 elements).

5. Drilling degrees of freedom and nonconforming modes

A good reason for using the drilling degrees of freedom in the plane stress/strain elements is found in modeling shells as an assembly of flat elements. In a typical finite element method, degrees of freedom allowed at each node consist of three translational displacements and three rotations. If flat shell elements which do not include drilling degrees of freedom are connected to a node where six degrees of freedom are assigned, then the drilling degree of freedom at that node is not resisted and the stiffness matrix becomes singular. This difficulty is neatly avoided by including drilling degrees of freedom in the element stiffness formulation.

There are several methods suggested to establish the plane stress element with drilling degrees of freedom (Cook 1986, Ibrahimbegovic, *et al.* 1990, MacNeal and Harder 1988, Yunus 1988, Choi and Lee 1995). The drilling degrees of freedom for these elements are associated with the parabolic shaped deformation of the element sides (See Fig. 15). When these parabolic modes are applied to the displacement interpolation, the deformation of the element side can not be fully expressed by nodal rotations only since the deformation in the tangential direction of element side needs to be better approximated by additional displacement mode. Thus, the normal compo-

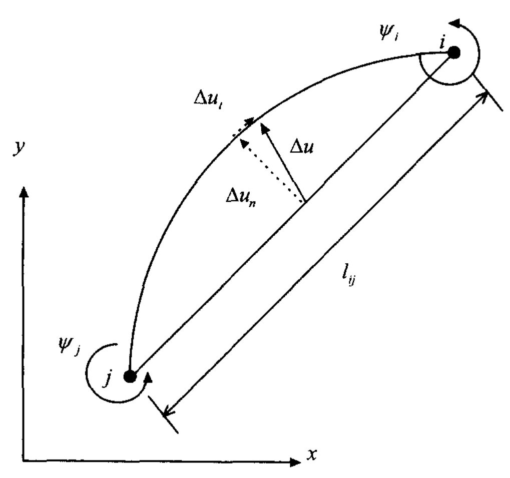

Fig. 15 Side displacement produced by drilling degrees of freedom.

Table 8 Tip displacement of Cook's problem

Element	Nodes/element	2×2 mesh	4×4 mesh	Remarks
Q4	4	11.845	18.299	basic 4-node element
Ibrahimbegovic *et al.* (1990)	4	20.683	23.668	w/ bubble mode
CLM-1 Choi and Lee (1995)	4	19.442	22.734	w/o tangential non-conforming modes
	5	19.669	22.863	
	6	20.932	23.133	
	7	22.967	23.577	
CLM-2 Choi and Lee (1995)	4	19.689	22.816	w/ tangential non-conforming modes
	5	19.877	22.953	
	6	21.120	23.205	
	7	23.334	23.694	
Reference value*	-	23.91		-

*Reference value is obtained from a fine mesh

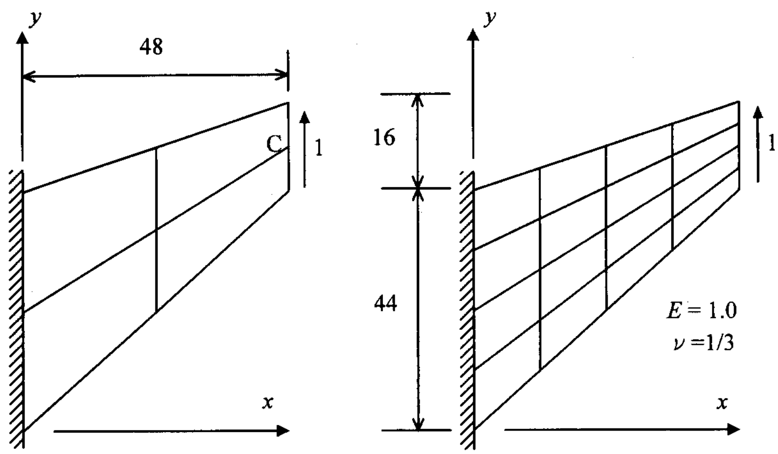

Fig. 16 Cook's membrane.

nents of the mid-side displacements is expressed by the nodal rotations

$$\Delta u_n = N^{side}(\xi,\ \eta)\,\frac{l_{ij}}{8}\,(\Psi_i - \Psi_j) \tag{19}$$

and the tangential components of the mid-side displacements are retained as nonconforming modes. In these formulation, the normal component of displacement along the element side acts like the additional nonconforming mode and the retained tangential nonconforming modes are used as another tool for improving the behavior of the element.

The displacement field of the transition membrane element is defined as

$$\begin{bmatrix} u \\ v \end{bmatrix} = \sum N_i\ \boldsymbol{u}_i + \sum \boldsymbol{\Delta u}_{ni}\ \boldsymbol{n}_i + \sum \Delta\,\bar{\boldsymbol{u}}_{tj}\,\boldsymbol{t}_j + N_o \boldsymbol{\Delta u}_o \tag{20}$$

where $\boldsymbol{\Delta u}_n$ is defined in Eq. (19), $\boldsymbol{\Delta \bar{u}}_t$ is tangential component of the mid-side displacements by nonconforming modes, N_o is the bubble mode, $\boldsymbol{n}_i$ and $\boldsymbol{t}_j$ are normal and tangential vectors to the corresponding side (Choi and Lee 1995). The inplane transition element which does not have tangential nonconforming modes is denoted as CLM-1 and the element which has tangential nonconforming modes is denoted as CLM-2.

The numerical results of the membrane problem in Fig. 16 solved by the original variable node membrane element with drilling degrees of freedom (CLM-1) and that of the element with additional tangential modes (CLM-2) are listed in Table 8. It is shown that the addition of tangential nonconforming modes also improve the behavior of the element with drilling degrees of freedom.

Choi and Lee (1996) also established variable node transition flat shell element with drilling degrees of freedom as a combination of the variable node membrane element CLM (Choi and Lee 1995) and the variable node plate with substitute shear strain fields (Choi and Park 1992).

6. Conclusions

A state-of-the-art on the development of a series of finite elements by the addition of nonconforming displacement modes is presented. The general behavior of these nonconforming plate and shell finite elements ranging from four to eight node elements is best improved by the combined use of the addition of nonconforming modes, the application of reduced (or selective) integration, and construction of substitute shear strain fields even though the individual schemes can improve the behavior of the elements to some extent. The improvement is attributable to the fact that the merits of each technique are merged into the formation of new elements in a complementary manner.

When the elements are formulated by the combined use of the multiple improvement techniques, it was also shown that these elements give the reliable solutions without any defect such as locking and spurious zero energy modes for linear as well as nonlinear benchmark problems.

Among these nonconforming elements, NC-QH and NC8-DC showed the best performances in 8-node degenerated plate/shell elements. The improvement obtained for 4-node element by addition of nonconforming modes was more significant than that obtained for 8-node element. However, the 4-node element still need to be improved further to become an effective element for the practical use.

The behavior of the transition elements with variable node can also be improved by the addition of nonconforming displacement modes in the same manner that an element without variable node is improved. There are no problems associated with locking and spurious zero energy modes in the behavior of the transition elements for moderately thick plate. These transition elements with a variable number of nodes are more versatile and can be effectively used in the adaptive mesh refinement in practical problems.

To formulate a new versatile transition flat shell element incorporating the concept of nonconforming modes, the combination of a variable node transition membrane element with drilling degrees of freedom (CLM) and transition plate bending element was also suggested.

The concept of the combined use of the different improvement schemes discussed in the present paper can be applied to the three-dimensional problems which is beyond the scope of this paper.

References

Ahmad, S., Irons, B.M. and Zienkiewicz, O.C. (1970), "Analysis of thick and thin shell structures by curved finite elements", *Int. J. Numer. Methods Eng.*, **2**, 419-451.

Bathe, K.J., Wilson, E.L. and Peterson, F.E. (1974), "SAP IV-A Structural Analysis Program for Static and Dynamic Response of Linear Systems", *Earthquake Engineering Research Center Report No. EERC 73-11*, University of California, Berkeley, California, June 1973, revised April.

Choi, C.K. and Schnobrich, W.C. (1975), "Nonconforming finite element analysis of shells", *J. Eng. Mech. Div. ASCE*, **101**, 447-464.

Choi, C.K. (1982), "General shell analysis by the nonconforming finite element", *Bull. Int. Ass. Shell and Spatial Struct.*, **80**, 5-16.

Choi, C.K. (1984), "A conoidal shell analysis by modified isoparametric element", *Comp. Struct.*, **18**, 921-924.

Choi, C.K. (1986), "Reduced integrated nonconforming plate element", *J. Eng. Mech. Div. ASCE*, **112**, 370-385.

Choi, C.K. and Kim, S.H. (1988), "Reduced integration, nonconforming modes, and their coupling in thin plate elements", *Comp. Struct.*, **29**, 57-62.

Choi, C.K. and Kim, S.H. (1989), "Coupled use of reduced integration and nonconforming modes in quadratic Mindlin plate element", *Int. J. Numer. Methods Eng.*, **28**, 1909-1928.

Choi, C.K. and Park, Y.M. (1989), "Nonconforming transition plate bending elements with variable midsides nodes", *Comp. Struct.*, **32**, 295-304.

Choi, C.K. and Kim, S.Y. (1989), "Nonconforming axisymmetric elements for the analysis of containment structures", *Tran. 10th Int. Conf. SMIRT*, California.

Choi, C.K. and Yoo, S.W. (1991a), "Combined use of multiple improvement techniques in degenerated shell element", *Comp. Struct.*, **39**, 557-569.

Choi, C.K. and Yoo, S.W. (1991b), "Geometrically nonlinear behavior of an improved degenerated shell element", *Comp. Struct.*, **40**, 785-794.

Choi, C.K. and Park, Y.M. (1992), "Transition plate bending elements for compatible mesh gradation", *J. Eng. Mech. Div. ASCE*, **118**, 462-480.

Choi, C.K. (1992), "Development of the nonconforming elements", *Proceedings of Korea-French Seminar on COMPUTATIONAL MECHANICS IN STRUCTURAL ENGINEERING*, July 7-9, 1992, France, 1-18.

Choi, C.K. and Lee, W.H. (1995), "Transition membrane elements with drilling freedom for local mesh refinements", *Struct. Eng. Mech.*, **3**, 75-89.

Choi, C.K. and Lee, W.H. (1996), "Versatile variable node flat shell element", *J. Eng. Mech. Div. ASCE*, **122**, 432-441.

Choi, C.K. and Park, Y.M. (1997), "Conforming and nonconforming transition plate bending elements for an adaptive *h*-refinement", *Thin-Walled Str.* **28**(1), 1-20.

Clough, R.W. and Johnson, C.P. (1968), "A Finite Element Approximation for Analysis of Thin Shells", *Int. J. of Solids and Structures*, **4**(1).

Cochet, J.F. and Dhatt, G.S. (1978), "Plasticity analysis by a nonconforming plane element", *Int. J. Numer. Methods Eng.*, **12**, 561-566.

Cook, R.D. (1972), "More on reduced integration and isoparametric elements", *Int. J. Numer. Methods Eng.*, **5**, 141-142.

Cook, R.D. (1974), "Improved two-dimensional finite element", *J. Struct. Div. ASCE*, 1851-1863.

Cook, R.D. (1975), "Avoidance of parasitic shear in plane element", *J. Struct. Div. ASCE*, 1239-1253.

Cook, R.D. (1986), "On the Allman triangle and a related quadrilateral element", *Comp. Struct.*, **22**, 1065-1067.

Fezans, G. and Verchery, G. (1982), "Some results on the behaviour of degenerated shell (D.S.) elements", *Nucl. Eng. Des.*, **70**, 27-35.

Gupta, A.K. (1978), "A finite element for transition from a fine to a coarse grid", *Int. J. Numer. Meth. Eng.*, **12**, 35-45.

Hinton, E. and Huang, H.C. (1986), "A family of quadrilateral Mindlin plate elements with substitute shear strain fields", *Comp. Struct.*, **23**, 409-431.

Huang, H.C. and Hinton, E. (1986), "A new nine node degenerated shell element with enhanced membrane and shear interpolation", *Int. J. Numer. Methods Eng.*, **22**, 73-92.
Hughes, T.J.R. and Cohen, M. (1978), "The heterosis finite element for plate bending", *Comp. Struct.*, **9**, 445-450.
Hughes, T.J.R., Cohen, M. and Haron, M. (1978), "Reduced and selective integration techniques in the finite element analysis of plates", *Nuclear Eng. Desgn.*, **46**, 203-222.
Hughes, T.J.R. and Tezduyar, T.E. (1981), "Finite elements based upon Mindlin plate bending theory with particular reference to the four-node bilinear isoparametric element", *J. Appl. Mech.*, **48**, 587-596.
Ibrahimbegovic, A., Taylor, R.L. and Wilson, E.L. (1990), "A robust quadrilateral membrane finte element with drilling degrees of freedom", *Int. J. Numer. Methods Eng.*, **30**, 445-457.
Kebari, H. and Cassel, A.C. (1991), "Stabilization by nonconforming modes : 9-node membrane element with drilling freedom", *Int. J. Numer. Methods Eng.*, **31**, 1453-1468.
Kim, S.H. and Choi, C.K. (1988), "Improved finite element models for the analysis of plate and shell structures", *SEMR88-01E*, Dept. Civil Eng., KAIST.
Kim, S.H. and Choi, C.K. (1992), "Improvement of quadratic finite element for Mindlin plate bending", *Int. J. Numer. Methods Eng.*, **34**, 197-208.
Lee, S.W. and Wong, S.C. (1982), " Mixed formulation finite elements for Mindlin theory plate bending", *Int. J. Numer. Methods Eng.*, **18**, 1297-1311.
MacNeal, R.H. and Harder, R.L. (1988), "A refined four-noded membrane element with rotational degrees of freedom", *Comput. Struct.*, **28**, 75-84.
Mindlin, R.D. (1951), "Influence of rotatory inertia and shear on flexural motions of isotropic elastic plates", *J. Appl. Mech.*, **18**, 31-38.
Parisch, H. (1979), "A critical survey of the 9-node degenerated shell element with special emphasis on thin shell application and reduced integration", *Comp. Methods Appl. Mech. Eng.*, **20**, 323-350.
Park, Y.M. and Choi, C.K. (1997), "The patch tests and convergence for nonconforming Mindlin plate bending elements", *Struct. Eng. Mech.*, **5**, 471-490.
Pawsey, S.F. and Clough, R.W. (1971), "Improved numerical integration of thick shell finite elements", *Int. J. Numer. Methods Eng.*, **3**, 575-586.
Pugh, E.D.L., Hinton, E. and Zienkiewicz, O.C. (1978), "A study of quadrilateral plate bending elements with reduced integration", *Int. J. Numer. Methods Eng.*, **12**, 1059-1079.
Surana, K.S. (1983), "Geometrically nonlinear formulation for the curved shell elements", *Int. J. Numer. Methods Eng.*, **19**, 581-615.
Sze, K.Y. and Chow, C.L. (1991), "An incompatible element for axisymmetric structure and its modification by hybrid method", *Int. J. Numer. Methods Eng.*, **31**, 385-405.
Taylor, R.L., Beresford, P.J. and Wilson, E.L. (1976), "A nonconforming element for stress analysis", *Int. J. Numer. Methods Eng.*, **10**, 1211-1219.
Timoshenko, S.P. and Woiniwsky-Krieger, S. (1959), Theory of Plates and Shells, 2nd ed., MaGraw-Hill, New York.
Tsach, U. (1981), "Locking of thin plate/shell elements", *Int. J. Numer. Methods Eng.*, **17**, 633-644.
Yunus, S.M. (1988), "A study of different hybrid elements with and without rotational D.O.F. for plane stress/plane strain problem", *Comp. Struct.*, **30**, 1127-1133.
Wilson, E.L., Taylor, R.L., Doherty, W.P. and Ghaboussi, J. (1971), "Incompatible displacement modes", *ONR Symposium on Numerical and Computer Methods in Structural Mechanics*, University of Illinois, Urbana.
Zienkiewicz, O.C., Taylor, R.L. and Too, J.M. (1971), "Reduced integration technique in general analysis of plates and shells", *Int. J. Numer. Methods Eng.*, **3**, 275-290.